Magnetostatic modes in Fibonacci magnetic and nonmagnetic multilayers

J. W. Feng, G. J. Jin, A. Hu, S. S. Kang, S. S. Jiang, and D. Feng
National Laboratory of Solid State Microstructures and Department of Physics, Nanjing University, Nanjing 210093, People's Republic of China
and Center for Advanced Studies in Science and Technology of Microstructures, Nanjing 210093, People's Republic of China
(Received 18 May 1995)

We study the magnetostatic modes in a Fibonacci multilayer consisting of alternating magnetic and nonmagnetic layers. The constant of motion, depending on both the in-plane wave vector and the frequency of the mode, is explicitly obtained and used to describe general features of the frequency spectra. Furthermore, spin wave spectra and precession amplitudes of magnetization for a finite Fibonacci multilayer are numerically calculated by the transfer matrix method. For a given in-plane wave vector, the distribution of frequency exhibits a triadic Cantor structure with large gaps in the low-frequency region, small gaps in the high-frquency region, and many "isolated" modes in the gaps. The gaps strongly depend on the in-plane wave vector and the thicknesses of the magnetic and nonmagnetic layers. We find three types of states in the quasiperiodic direction: extended states in the high-frequency region near the upper band edge, critical states in the triadic subbands, and surface states in gaps. Besides the conventional Damon-Eshbach surface mode localized at two opposite surfaces of the multilayer for positive and negative wave vectors, respectively, another kind of surface modes are discovered. When the wave vector is reversed, these modes are still localized at the same sides of the multilayer.

I. INTRODUCTION

One of the new rapidly developing areas of solid state physics is magnetic multilayers. There has been a considerable amount of work on the collective excitations in magnetic multilayers. Especially, magnetostatic modes, the spin waves in a magnetostatic limit, in periodic multilayers consisting of alternating magnetic and nonmagnetic layers, have been studied in more detail both experimentally and theoretically.[1–6] It turns out that only the Damon-Eshbach (DE) modes,[7] localized on the surfaces of single magnetic films, produce long-range dipolar fields outside of the films and hence interact to form bulk spin waves of the multilayer which have sinusoidal amplitudes across the multilayer. In addition, when the system is finite or semifinite, a surface spin wave of the multilayer, having the amplitude decreasing exponentially as one penetrating into the multilayer, exists if the thickness of magnetic layers is larger than that of nonmagnetic layers. This surface mode is often called the DE surface mode of the multilyer, and can be regarded approximately as the DE surface wave of a single-thick magnetic layer with thickness being the sum of all magnetic layers.

On the other hand, following the report in 1984 of the existence of a quasicrystalline phase in metallic alloys,[8] the electronic and phonon properties of one-dimensional quasiperiodic systems, known as the Fibonacci chains or Fibonacci multilayers, have attracted great interest from a theoretical viewpoint. It has been found that both electronic and phonon spectra of Fibonacci chains or Fibonacci multilayers are of Cantor-set structures and the corresponding eigenstates may be localized, extended, or critical.[9–15] Parallel to the theoretical development, the experimental investigations have been made in various aspects including diffraction,[16,17] superconductivity,[18] elasticity,[19] and Raman scattering.[16,20] However, so far only very little work[21] has been done on the magnetostatic modes in the Fibonacci magnetic multilayer (FMM). We consider it worthwhile to explore the properties of magnetostatic modes in such a magnetic multilayer, since spin waves in a range of wave vectors ($k \approx 10^5$ cm^{-1}) are experimentally accessible in Brillouin light-scattering experiments.

In this paper, the electromagnetic boundary conditions in the magnetostatic limit are applied to match the magnetic potentials in various layers. The recursion relations are obtained and numerically solved by transfer matrix method for finite Fibonacci multilayers. In Sec. II, we derive the recursion equations and the expression of motion constant, and give out the basic formula for numerical calculation. In Secs. III and IV, we present our calculating results about frequency spectra and amplitudes, respectively. Finally we discuss some experimental aspects about FMM in Sec. V.

II. THEORY

A. Recursion relations

A FMM in the present study is constructed by two blocks, A and B, according to the following relations:

$$S_{j+1}=\{S_j,S_{j-1}\}, \quad S_1=A, \quad S_2=AB.$$

Each of blocks, A or B, consists of a magnetic film with equal thickness d and a nonmagnetic film with thickness d_1 for block A and d_2 for block B.

We discuss here only the magnetostatic spin waves whose wave vector $\mathbf{k}$, parallel to the sample plane, is perpendicular to the static field $\mathbf{H_0}$ which is also applied in the sample plane (the Voigt geometry). We introduce a coordinate system in such a way that the wave vector $\mathbf{k}$ is along the y direction, the external field $\mathbf{H_0}$ and saturation magnetization $\mathbf{M}_s$ are along the z direction and the normal of the film along the x axis. The intersections of midplanes of the magnetic

films with the x axis are x_l ($l=1,2,3,\ldots$) with $x_1=0$. Generally, the magnetic potential of the multilayers has the following form:[2–4]

$$\Psi(x,y)=X(x)\exp(iky). \tag{1}$$

Following Grünberg,[3] we write X inside the lth magnetic layer

$$X^{\text{in}}(x)=g_l\exp[Q(x-x_l)]+h_l\exp[-Q(x-x_l)] \tag{2}$$

and inside the lth nonmagnetic layer

$$X^{\text{ext}}(x)=p_l\exp[Q(x-x_l)]+q_l\exp[-Q(x-x_l)], \tag{3}$$

where Q is positive and $Q=\pm k$. Applying the boundary conditions at the interfaces between magnetic and nonmagnetic layers

$$\Psi^{\text{in}}=\Psi^{\text{ext}}, \tag{4}$$

$$(1+\kappa)\frac{\partial\psi^{\text{in}}}{\partial x}-i\nu\frac{\partial\psi^{\text{in}}}{\partial y}=\frac{\partial\psi^{\text{ext}}}{\partial x}, \tag{5}$$

where

$$\kappa=\frac{\Omega_H}{\Omega_H^2-\Omega^2},\quad \nu=\frac{\Omega}{\Omega_H^2-\Omega^2},$$

$$\Omega_H=\frac{H_0}{4\pi M_s},\quad \Omega=\frac{\omega}{4\pi\gamma M_s},$$

M_s is the saturation magnetization, γ the gyromagnetic ratio, and ω is the frequency, the coefficients p_l and q_l in the nonmagnetic layer can be eliminated, and the coefficients g_l, h_l, g_{l+1}, and h_{l+1} of two adjacent magnetic layers are correlated by

$$\begin{pmatrix} g_{l+1} \\ h_{l+1} \end{pmatrix}=M(l)\begin{pmatrix} g_l \\ h_l \end{pmatrix}, \tag{6}$$

where $M(l)$ is a transfer matrix. For our model, $M(l)$ only has two different forms, $M(1)$ and $M(2)$, and their explicit forms are given as follows:

$$M(i)=\begin{pmatrix} a(i) & b(i) \\ c(i) & d(i) \end{pmatrix},\quad i=1,2, \tag{7}$$

$$a(i)=\{-[\nu^2-(\kappa+2)^2]\exp(2Qd+Qd_i)+(\nu^2-\kappa^2)\exp(2Qd-Qd_i)\}/c,$$

$$b(i)=(\pm\nu-\kappa)(\pm\nu-\kappa-2)\{-\exp[Q(d+d_i)]+\exp[Q(d-d_i)]\}/c,$$

$$c(i)=(\pm\nu+\kappa)(\pm\nu+\kappa+2)[\exp(Qd+Qd_i)-\exp(Qd-Qd_i)]/c,$$

$$d(i)=\{[-\nu^2+(\kappa+2)^2]\exp(-Qd_i)+(\nu^2-\kappa^2)\exp(Qd_i)\}/c,$$

$$c=4(\kappa+1)\exp(Qd),$$

where the upper (lower) sign is for the positive (negative) value of the wave vector. It can be proved that both $M(1)$ and $M(2)$ are unimodular. Using the products of matrices we have

$$\begin{pmatrix} g_{l+1} \\ h_{l+1} \end{pmatrix}=M(l)M(l-1)\cdots M(1)\begin{pmatrix} g_1 \\ h_1 \end{pmatrix}. \tag{8}$$

We define $\underline{M}_j=M(F_j)M(F_j-1)\cdots M(1)$, where F_j is the jth Fibonacci number. Then the following recursion relation for $\underline{M}_j$ can be obtained:

$$\underline{M}_j=\underline{M}_{j-2}\underline{M}_{j-1},\quad (j>2) \tag{9}$$

with the initial condition

$$\underline{M}_1=M(1),\quad \underline{M}_2=M(2)M(1). \tag{10}$$

The recursion relation (9) together with (10) defines a nonlinear dynamical map and gives a powerful calculation scheme.

B. Constant of motion

Similar to the method used in dealing with electronic and phonon problems,[9,12] by defining $x_j\equiv\frac{1}{2}\text{tr}\underline{M}_j$, the recursion relation for x_j reads

$$x_{j+1}=2x_jx_{j-1}-x_{j-2}. \tag{11}$$

This relation leads to the result that the quantity

$$I=x_{j+1}^2+x_j^2+x_{j-1}^2-2x_{j+1}x_jx_{j-1}-1 \tag{12}$$

is a constant of motion on successive iterations and this constant reflects the strength of the effect of quasiperiodicity. From (9)–(12), I could be explicitly deduced as

$$I=\frac{(\Omega_H+\frac{1}{2})^2-\Omega^2}{4(\Omega_H^2+\Omega_H-\Omega^2)^2}\sinh^2(Qd)\sinh^2[Q(d_1-d_2)]. \tag{13}$$

Clearly, this expression is different from the expressions of I for the electronic and phonon problems[9] of Fibonacci chains. Not only does the quantity I depend on reduced frequency Ω, but also on in-plane wave vector k ($Q=|k|$). When $d_1=d_2$, $I=0$, the system is recovered to a periodic multilayer. According to Komoto *et al.*,[9] the structure of frequency spectra including widths of bands and gaps is determined by the quantity I. A large I implies a large gap while a small I corresponds to a small gap. Thus from the Ω and k dependence of quantity I, we can discuss general features of the frequency distribution. For the present FMM model, the reduced frequency Ω is limited to the range

$$\sqrt{(\Omega_H^2+\Omega_H)}<\Omega<\Omega_H+1/2. \tag{14}$$

In this possible fequency range, quantity I is always positive if $d_1\neq d_2$. Quantity I increases with decreasing Ω for a given wave vector k and increases with k increasing for a given frequency. Thus the scaling of the frequency band is not uniform. Frequency spectra have small gaps in the high-frequency and small wave vector region. When $\Omega\to\Omega_H+1/2$, $I\to 0$ corresponds to a zero gap. Thus near this frequency, it is expected to obtain some extended states.

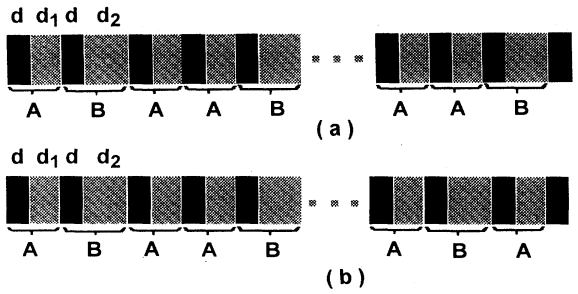

FIG. 1. Model of a finite FMM, (a) even j and (b) odd j.

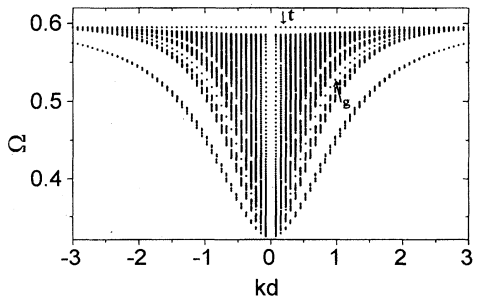

FIG. 2. Dispersion relations of a FMM with $N=611$, $d=50$ nm, $d_1=40$ nm, and $d_2=20$ nm for both positive and negative wave vectors. "t" and "g" represent a top "isolated" branch and a gap "isolated" branch, respectively.

On the other hand, when $\Omega\rightarrow\sqrt{(\Omega_H^2+\Omega_H)}$, $I\rightarrow\infty$, and quasiperiodic features including frequency and amplititude distributions are expected to be the most obvious. This result, compared to that of the phonon where I increases with frequency ($I\propto\omega^4$), seems somewhat surprising, but it is resonable indeed. Considering magnetostatic modes of periodic multilayers is helpful for us to understand the present result. In the periodic magnetic multilayers,[3] the high-frequency mode implies a long-wavelength wave with a real wave vector normal to the film and the wavelength becomes shorter with frequency decreasing. Thus in the high-frequency region, the frequency of the mode, due to its long wavelength, is relatively insensitive to the local arrangements of magnetic and nonmagnetic layers, and the behavior of spin waves in FMM, on the average, is similar to that in periodic multilayers.

C. Basic calculation formula for a finite FMM

A finite FMM studied here is made up of F_j blocks arranged in the Fibonacci sequence and an additional magnetic layer of thickness d at right boundary (see Fig. 1). Thus all N ($N=F_j+1$) magnetic films are seperated by F_j nonmagnetic films. In this case, we can get two different configurations at the right boundary, depending on odd or even number j (see Fig. 1).

The eigenequations for a finite FMM consist of (8) and following two equations:

$$(\pm\nu+\kappa)g_1+(\pm\nu-\kappa+2)\exp(kd)h_1=0, \quad (15a)$$

$$(\pm\nu+\kappa+2)\exp(kd)g_N+(\pm\nu-\kappa)h_N=0, \quad (15b)$$

which come from the boundary conditions at the left and right surfaces of the system. Using the condition that the equations have nontrivial solutions and applying a numerical calculation, we can obtain the spectra of spin waves. Furthermore, the precession amplitudes m_x and m_y of magnetization in the lth magnetic layer are given by[2,3,7]

$$m_x=\frac{1}{4\pi}\{(\pm\nu Q+\kappa Q)g_l\exp[Q(x-x_l)] +(\pm\nu Q-\kappa Q)h_l\exp[(-Q(x-x_l)]\}, \quad (16a)$$

$$m_y=\frac{1}{4\pi}\{(\nu Q\pm\kappa Q)g_l\exp[Q(x-x_l)] +(-\nu Q\pm\kappa Q)h_l\exp[-Q(x-x_l)]\}, \quad (16b)$$

where the coefficients g_l and h_l can be calculated through Eqs. (8) and (15a).

For numerical calculation, we select an Fe/Cu FMM and take the magnetic parameters of bulk Fe given in the literature:[3] $4\pi M_s=21\,000$ G, $\gamma=1.85\times10^{11}$ sec^{-1}, and $H_0=2000$ G.

III. SPECTRA

Figure 2 shows the dispersion relations of a FMM with $N=611$, $d=50$ nm, $d_1=40$ nm, $d_2=20$ nm. From Fig. 2, it can be seen that the spectrum consists of bandlike densed branches and "isolated" branches. The frequency of top "isolated" branch (see Fig. 2) does not depend on k while the frequences of other "isolated" branches in gaps obviously are k dependent. Also, for a given in-plane wave vector k, the distribution of frequencies exhibits the character of subbands. For intermediate values of $|k|$, subbands are most obvious, and hence the effect of quasiperiodicity is strongest. As $|k|$ decreases, the band becomes relatively uniform and the feature of quasiperiodicity is not obvious, since small $|k|$ corresponds to small I. For large $|k|$, the frequencies degenerate and the band becomes narrow, which reduces the effect of I, thus the effect of quasiperiodicity is also not obvious.

In order to understand frequency distribution of states in details, we calculate eigenfrequencies of the system with $N=2585$, $d=50$ nm, $d_1=40$ nm, $d_2=20$ nm for $k=1.5\times10^5$ cm^{-1}. Figure 3 shows the frequency distribution with mode number. A hierarchy of gaps and many "isolated" states in gaps can clearly be seen. The low-frequency regime is self-similar, having a Cantor-set-like structure. There every band has two gaps giving rise to three subbands, each one of them having two gaps and so on. In the high-frequency case, the number of gaps and their size tend to zero. The characters of frequency spectra are consistent with that described by the quanity I.

Figures 4 and 5 show the variations of reduced frequency distributions with the ratio d/d_1 for given $k=1.875\times10^5$

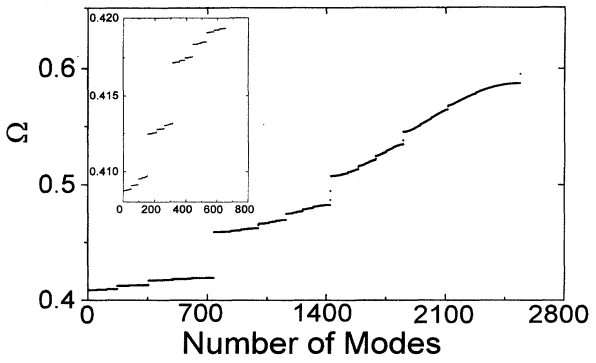

FIG. 3. Frequency spectrum, reduced frequency Ω vs mode number for a FMM with $N=2585$, $d=50$ nm, $d_1=40$ nm, $d_2=20$ nm, and $k=1.5\times 10^5$ cm^{-1}. The inset shows an enlarged region.

cm^{-1}, $d_1=40$ nm, and $d_2=20$ nm, and with the ratio d_2/d_1 for given $k=1.5\times 10^5$cm^{-1}, $d=50$ nm, and $d_1=40$ nm, respectively. The general feature is that the whole band can be regarded as made up of two, three, or four mainbands, which depends on the thicknesses of magnetic and nonmagnetic layers, and each main band consists of three subbands. As for "isolated" states, two important features should be emphasized. First, their appearance is closely related to the parameters d, d_1, and d_2. When these parameters vary, some of "isolated" states can be transformed into subband states. Second, the top "isolated" state behaves differently from "isolated" states in gaps. When $d>d_1,d_2$, the top "isolated" state appears and its frequency almost does not vary with the above parameters, but the frequences of the "isolated" states in gaps are obviously dependent on them. This result indicates that the top mode is not sensitive to the details of magnetic and nonmagnetic arrangements to which "isolated" states in gaps are.

In fact, the present "isolated" states correspond to surface states of the multilayer. Through decoupling analysis, we can get more details about them. For example, an "isolated" state labelled by "s" in Fig. 5 arises from the effect of additional magnetic layer at the right boundary. When $d_2\to\infty$, the system decouples into three kinds of configurations [referring Fig. 1(a)]: degenerate magnetic trilayers separated by two nonmagnetic layers, degenerate magnetic bilayers separated by a nonmagnetic layer, and a nondegenerate single-magnetic layer located at right boundary. Thus in the limit of $d_2\to\infty$ the frequency of additional magnetic layer does not generate with frequencies of the other magnetic configurations. On the other hand, if $d_1\to\infty$, the multilayer decouples into two highly degenerate configurations: magnetic bilayers and single layers, respectively. In this case, the right magnetic layer together with its nearest magnetic layer makes up magnetic bilayers, and their frequencies degenerate with the ones of the magnetic bilayers inside the multilayer (see inset in Fig. 5).

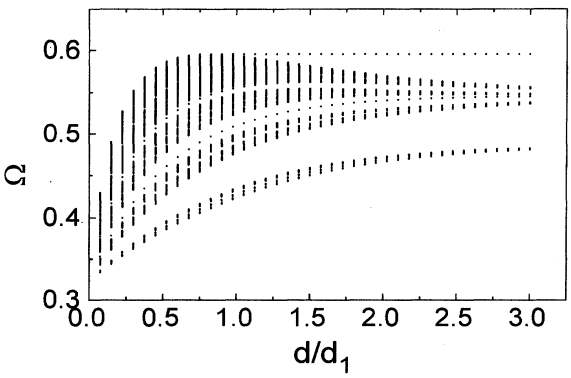

FIG. 4. The variation of reduced frequency distributions with the ratio d/d_1 for given $k=1.875\ 10^{-5}$ cm^{-1}, $d_1=40$ nm, and $d_2=20$ nm.

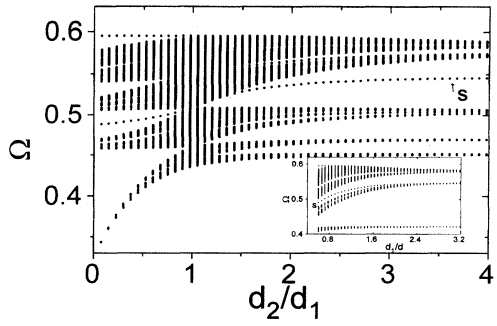

FIG. 5. The variation of frequency distribution with the ratio d_2/d_1 for given $k=1.5\times 10^5$ cm^{-1}, $d=50$ nm, and $d_1=40$ nm.

For a FMM, the arrangements of magnetic and nonmagnetic layers on both right and left boundaries are asymmetric, thus the frequencies of left and right surface modes are nondegenerate except for top surface mode. Also, as described in Sec. II, two different configurations exist at the right boundary, depending on the odd or even generation number j of the Fibonacci sequence. It leads to the frequencies of right surface modes being sensitive only to the even or odd j to which the frequencies of left surface modes are insensitive if Fibonacci numbers F_j are adequately large. By using these properties, we can distinguish right surface (RS) modes from left ones (LS) except for top surface mode. These characters are clearly illustrated in Fig. 6.

IV. PROPERTIES OF STATES

For showing the properties of the magnetostatic modes, we take the precession amplitudes m_x and m_y to describe magnetic states of a FMM and we find that the distributions of m_x and m_y are similar. For simplicity, we only give the calculating results of m_x below. In general, there exist three types of magnetostatic modes in a finite FMM: surface localized, extended, and critical modes.

A. Surface modes

As mentioned in Sec. III, "isolated" modes are surface ones. In the present finite FMM, we find two different kinds of surface modes. The top "isolated" mode is a DE mode of the multilayer with amplitudes exponentially decaying from

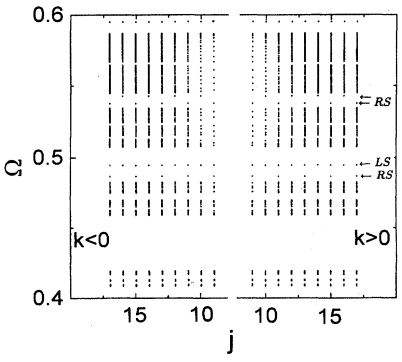

FIG. 6. Frequencies vs the Fibonacci generation number j of a FMM with $d=50$ nm, $d_1=40$ nm, $d_2=20$ nm, and $k=\pm 1.5\times 10^5$ cm^{-1}. The "isolated" states with their frequencies independent of j are left surface (LS) modes except for the top "isolated" mode, while the "isolated" states that appear only for even or odd j correspond to the right surface modes (RS).

a surface, simliar to the DE surface mode of a single magnetic layer with thickness Nd . The precession is both circular and in phase throughout the multilayer. Thus its frequency is almost independent of the thicknesses of magnetic and nonmagnetic layers for $d>d_1,d_2$. Furthermore, this mode is unreciprocal. The mode has its maximum amplitudes at the right surface of multilayer for positive k and at the opposite surface for negative k. The result is shown in Fig. 7(a). However, the "isolated" states in gaps are the new surface modes of the multilayer which are different from the conventional DE surface mode of the periodic multilayers. First, the amplitudes of new modes are oscillation damping from the outermost magnetic layers (in each layer their amplitudes still exponentially decaying) [see Fig. 7(b)]. The precession is both elliptic and out of phase in adjacent magnetic layers. Therefore, the frequency of the precession is sensitive to the configurations of the magnetic and nonmagnetic layers at boundaries and depends on the thicknesses of magnetic and nonmagnetic layers as well as the value of in-plane wave vector. Another important difference is that the new surface modes are still localized at the same sides of the multilayer even though the in-plane wave vector is reversed.

B. Extended modes

For the frequencies near the top edge of the band, the corresponding states are extended due to the small constants of motion and the long wavelengths. Figure 8 shows the distributions of precession amplitudes in the midplane of each magnetic layer with the position of magnetic layer l. From Fig. 8, it can be seen that aperiodic amplitudes are modulated by a sinelike wave. Thus, on the whole, the system behaves mainly as for the ordinary periodic multilayers. As frequency decreases from the top band edge, the modulation wavelength descreases approximately following the relation $\lambda_\perp=2D/n$ $(n=1,2,3,\ldots)$ where D is the total thickness of a FMM. This behavior is very similar to the case of periodic magnetic multilayers.[3] The effect of aperiodicity can be further supressed if the frequency of the mode in the top subband $\rightarrow \Omega_H+1/2$, corresponding to $I\rightarrow 0$.

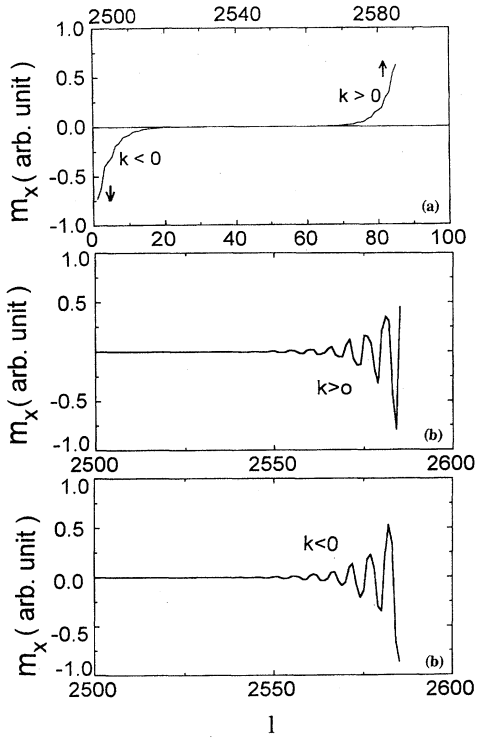

FIG. 7. m_x at midplane of each magnetic layer vs position labeled by l for two different kinds of surface- modes in a FMM with $N=2585$, $d=50$ nm, $d_1=40$ nm, and $d_2=20$ nm: (a) DE surface mode localized at right or left boundary with $\Omega=0.595\ 302\ 337\ 4$ corresponds to $k=\pm 1.5\times 10^5$ cm^{-1} and (b) the surface-mode localized at the same side of the FMM with $\Omega=0.486\ 782\ 467\ 5$ corresponds to $k=\pm 1.5\times 10^5$ cm^{-1}.

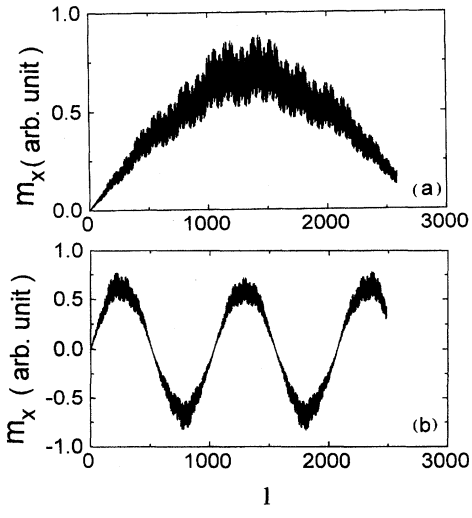

FIG. 8. Extended states of a FMM for given $N=2585$, $d=50$ nm, $d_1=40$ nm, $d_2=20$ nm, and $k=1.5\times 10^5$ cm^{-1}: (a) and (b) correspond to $\Omega=0.587\ 098\ 268\ 1$ (top band edge) and $\Omega=0.587\ 094\ 108\ 5$, respectively.

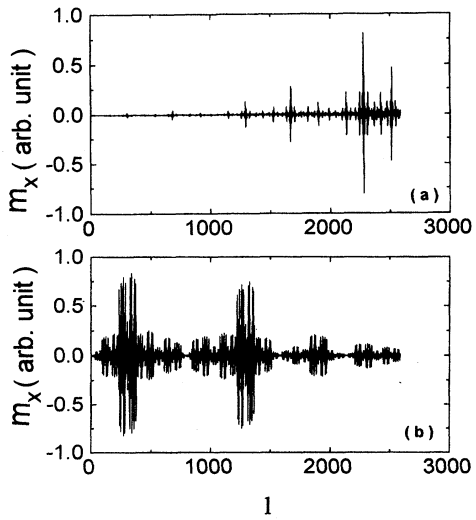

FIG. 9. Critical states of a FMM with $N=2585$, $d=50$ nm, $d_1=40$ nm, $d_2=20$ nm, and $k=1.5\times10^5$ cm^{-1}: (a) and (b) correspond to $\Omega=0.408\ 793\ 051\ 5$ and $\Omega=0.408\ 758\ 142\ 6$ (low band edge), respectively. The distributions of m_x indicate localization of states, but m_x is not exponentially decaying with l.

C. Critical modes

The same as the electronic and phonon problems, we find that in the case of magnetostatic modes most of the states are critical, especially in the low-frequency region where triadic subbands are most obvious. Figures 9(a) and 9(b) show the distributions of the precession amplitude m_x at midplane of each magnetic layer with the position of magnetic layer l. It is noted that the distributions of magnetization are neither sine extending nor exponentially decaying, but power-law decaying over the length of the system (critical states).

V. DISCUSSION AND CONCLUSION

We would like to discuss some experimental aspects about FMM. The spin waves in periodic magnetic multilayers have widely been studied with Brillouin light scattering in various systems such as Ni/Mo, Co/Ni, Fe/Pd, and Fe/W.[1,22–24] The multilayer with the Fibonacci sequence considered here may be fabricated by molecular beam epitaxy and sputtering techniques, and the spectra of spin waves can also be studied with Brillouin light scattering. In order to obtain the spectra showing the typical features of the Fibonacci sequence by Brillouin light scattering most effectively, choosing adequate thickness of magnetic and nonmagnetic layers is crucially important, since in Brillouin light-scattering experiments the values of k observed are on the order of 10^5 cm^{-1}. From our calculation on Fe/Cu FMM, d can be chosen according to the relation $kd\approx0.4-1$, since in this wave vector range the triadic spectra are most obvious. Moreover, two different kinds of surface modes can be distinguished through reversal of the external field or Stokes and anti-Stokes scattering in Brillouin light-scattering experiments.

In summary, we study some features of magnetostatic modes in a FMM. It is found that the structure of a band is strongly dependent on both in-plane wave vector and frequency of the mode. For a given intermediate value of a wave vector, the spectrum exhibits a triadic Cantor structure with nonuniform scaling. In the low-frequency region, there are large gaps and narrow bands in which the states are critical, whereas in the high-frequency region near the top band edge, the spectrum and precession amplitude behave mainly as for the ordinary periodic magnetic multilayers. Besides, the existence of two different kinds of surface modes in a finite FMM is predicated. The results presented here are expected to be observable experimentally and we hope this paper will stimulate experimental studies on such a system.

ACKNOWLEDGMENTS

This work is supported by the National Natural Science Foundation of China and the Provincial Natural Science Foundation of Jiangsu.

[1] M. Grimsditch, M. R. Khan, A. Hueny, and I. K. Schuller, Phys. Rev. Lett. **51**, 498 (1983).
[2] R. E. Camley, T. S. Rahman, and D. L. Mills, Phys. Rev. B **27**, 261 (1983).
[3] P. Grünberg and K. Mika, Phys. Rev. B **27**, 2955 (1983); P. Grünberg, M. G. Cottam, W. Vach, C. Mayer, and R. E. Camley, J. Appl. Phys. **45**, 456 (1982).
[4] J. Barnas, J. Phys. C **21**, 1021 (1988).
[5] R. Emtage and M. Daniel, Phys. Rev. B **29**, 212 (1983).
[6] H. K. Sy and Feng Chen, Phys. Rev. B **50**, 3411 (1994).
[7] R. W. Damon and J. R. Eshbach, J. Phys. Chem. Solids **19**, 308 (1961).
[8] D. Scechtman, I. Blech, D. Gratias, and J. W. Cahn, Phys. Rev. Lett. **53**, 1951 (1984).
[9] M. Komoto, L. P. Kadanof, and C. Tang, Phys. Rev. Lett. **50**, 1870 (1983); M. Komoto and J. R. Banavar, Phys. Rev. B **34**, 563 (1986).
[10] S. Ostlund, D. Pandit, H. J. Schellnhuber, and E. D. Siggia, Phys. Rev. Lett. **50**, 1873 (1983).
[11] Y. Liu and R. Riklund, Phys. Rev. B **35**, 6034 (1987).
[12] F. Nori and J. P. Rodriguez, Phys. Rev. B **34**, 2207 (1986).
[13] Jiang Ping Lu, Takashi Odagaki, and Joseph L. Birman, Phys. Rev. B **33**, 4809 (1986).
[14] V. Kumar and G. Ananthakrishna, Phys. Rev. Lett. **13**, 1476 (1987).
[15] T. Odagaki and L. Friedman, Solid State Commun. **57**, 12 (1986).
[16] R. Merlin, K. Bajema, R. Clarke, F-Y. Juang, and P. K. Bhacharya, Phys. Rev. Lett. **55**, 1157 (1985).
[17] A. Hu, C. Tien, X. J. Li, Y. H. Wang, and D. Feng, Phys. Lett. A **119**, 313 (1986); R. W. Peng, An, Hu, S. S. Jiang, C. S. Zhang, and D. Feng, Phys. Rev. B **46**, 7816 (1992).
[18] M. G. Karkut, J. M. Triscone, D. Ariosa, and O. Fischer, Phys. Rev. B **34**, 4390 (1986).
[19] H. Xia, X. K. Zhang, A. Hu, S. S. Jiang, R. W. Peng, W. Zhang,

D. Feng, G. Carlotti, D. Fioretto, G. Socino, and L. Verdini, Phys. Rev. B **47**, 3890 (1992).
[20] X. K. Zhang, H. Xia, G. X. Cheng, A. Hu, and D. Feng, Phys. Lett. A **136**, 312 (1989).
[21] S. J. Xiong, J. Phys. C **20**, L167 (1987).
[22] G. Rupp, W. Wetting, W. Jantz, and R. Krishnan, Appl. Phys. A **37**, 73 (1985).
[23] B. Hillebrands, P. Baumgart, R. Mock, G. Gutherodt, A. Boufelfel, and C. M. Falco, Phys. Rev. B **34**, 9000 (1986).
[24] B. Hillebrands, A. Boufelfel, C. M. Falco, P. Baumgart, G. Guntherodt, E. Zirngiell, and J. D. Thompson, J. Appl. Phys. **63**, 3880 (1988).